Desalination and Water Treatment
www.deswater.com
doi: 10.1080/19443994.2015.1033476

57 (2016) 7898–7909
April

Taylor & Francis
Taylor & Francis Group

$Fe_2(MoO_4)_3$ as a novel heterogeneous catalyst to activate persulfate for Rhodamine B degradation

Yong-Sheng Lu, Zhan Wang, Yun-Feng Xu*, Qiang Liu, Guang-Ren Qian

School of Environmental and Chemical Engineering, Shanghai University, Shanghai 200444, China, emails: luys7174@shu.edu.cn (Y.-S. Lu), wangzhan0315@163.com (Z. Wang), Tel. +86 21 66137745; emails: yfxu@shu.edu.cn (Y.-F. Xu), qliu@shu.edu.cn (Q. Liu), grqian@shu.edu.cn (G.-R. Qian)

Received 3 December 2014; Accepted 19 March 2015

ABSTRACT

Iron molybdate ($Fe_2(MoO_4)_3$) was used as a novel heterogeneous catalyst to activate persulfate ($S_2O_8^{2-}$) for rhodamine B (RhB) degradation. Results indicated 10 mg/L RhB can be completely removed under the addition of 4 mM $S_2O_8^{2-}$ and 0.4 g/L $Fe_2(MoO_4)_3$ within 240 min. $Fe_2(MoO_4)_3$ can be repeatedly used for six cycles and showed high stability with Fe leaching amounts less than 2.9% in each run. Possible catalytic mechanism was proposed as follows: RhB degradation intermediate products such as hydroxybenzene, quinone compounds and organic compound radicals acted as electron transfer agents to reduce Fe^{3+} to Fe^{2+}, which reacted with persulfate to form Fe^{3+} creating the redox cycling of iron, the RhB and those intermediate products are oxidized directly by the molybdenum peroxo complexes which forming probably with MoO_4^{2-} and persulfate, and the synergy between Fe^{3+} and MoO_4^{2-} occurring the catalytic effect on the persulfate. Additionally, the major intermediates of RhB were identified according to GC/MS and the possible degradation pathway was proposed.

Keywords: $Fe_2(MoO_4)_3$ catalyst; Persulfate; Sulfate radical; Degradation

1. Introduction

Industrial productions produce a series of environmental problems such as wastewater containing organic contaminants. It is urgent to explore the effective processes for the treatment of organic pollutants. Fenton reagent in advanced oxidation processes (AOPs) has been widely applied [1,2]. However, the required acidic pH has limited the application of Fenton process for inhibiting hydrolysis of Fe^{3+}. Instead, AOPs based on sulfate radicals (SR-AOPs) have attracted great attention since $SO_4^{\cdot-}$ is more selective for oxidation at neutral pH than $^{\cdot}OH$ with the similar oxidation ability [3,4].

Persulfate (PS), with higher solubility and better stability than H_2O_2, has been proved to generate $SO_4^{\cdot-}$ activated by ultraviolet light [5], heating [6], or transition metal ion (such as Fe^{2+}) [7]. Nevertheless, some drawbacks existed in the above homogenous ways, such as the light filtering effect [8], consuming great amounts of heat and the metal ions as secondary pollution. To overcome the disadvantages of homogenous ways, the method of persulfate activation by

*Corresponding author.

Presented at the 7th International Conference on Challenges in Environmental Science and Engineering (CESE 2014) 12–16 October 2014, Johor Bahru, Malaysia

iron-containing heterogeneous catalyst has been attached importance as iron is a relatively affordable, non-poisonous reagent. Previous studies showed that persulfate had been activated by zero-valent iron [9], Fe_3O_4 [10,11], core–shell Fe-Fe_2O_3 [12], ferrous hydroxide [13], and iron sulfides [14] in heterogeneous mode. Fe(II) was found to be the most effective constituent in these catalysts. However, it was so easy to be oxidized that the ferrous-containing catalysts were difficult to be preserved and reused. Therefore, it is necessary to develop the iron-containing heterogeneous catalysts with better stability and reproducibility.

$Fe_2(MoO_4)_3$ had been used as heterogeneous catalyst to activate H_2O_2 for the effective removal of acid orange II in wide range of pH because of Mo-containing systems with low PZC values (point of zero charge) [15,16], and MoO_4^{2-} could react with H_2O_2 to form molybdenum (Mo) peroxo complex, which is a strong oxidant and can oxidize the organic compounds [17]. Moreover, H_2O_2 and $S_2O_8^{2-}$ both have –O–O– bond in their structure, and it has been proposed that $Fe_2(MoO_4)_3$ could be suitable catalyst for persulfate activation.

In the present work, $Fe_2(MoO_4)_3$ was prepared by co-precipitation and activated persulfate for rhodamine B (RhB) removal. This study aimed to (1) investigating the characterizations and activating ability of $Fe_2(MoO_4)_3$, (2) surveying experimental parameters including RhB initial concentration, PS and $Fe_2(MoO_4)_3$ concentration, and pH value, (3) identifying the reactive radicals for the degradation and possible activation mechanism to persulfate, and (4) exploring the possible degradation pathway of RhB.

2. Materials and methods

2.1. Materials

RhB was purchased from Sinopharm Chemical Reagents (Shanghai, China). So did the following reagents: ammonium molybdate(VI) tetra-hydrate, iron(III) nitrate mono-hydrate, ammonium hydroxide (25%, w/v), molybdenum(VI) oxide, and iron(III). Potassium persulfate (PS) was from Aladdin Company. All those reagents used in this experiment were of analytical grade. All solutions were prepared with double-distilled water (DDW). And the pH of solution was adjusted with 0.05 mol/L H_2SO_4 or NaOH.

2.2. Synthesis and characterization of catalyst $Fe_2(MoO_4)_3$

According to the previous literatures [18,19], $Fe_2(MoO_4)_3$ catalyst was synthesized by co-precipitation as the following procedures. Firstly, 5 mL ammonium hydroxide with 1 M was added into the solution of 100 mL 0.005 M ammonium molybdate, then adding iron titrate (50 mL, 0.0465 M) into the mixed solution under vigorous agitation in 20 min at room temperature (25℃), and the solution continued to be vigorously stirred for 2 h and centrifuged. The precipitate obtained was washed with double-distilled water for several times and then drying at 80℃ for 12 h. Finally, the dried solid was calcined at 550℃ (2℃/min rate) for 2 h in environmental air.

The X-ray diffraction (XRD) patterns of all the synthesized $Fe_2(MoO_4)_3$ were determined on a X-ray diffractometer (Rigaku D/Max-2200X) using Cu Kα source. Fourier transform infrared spectra (FTIR) were collected from 500 to 4,000 cm^{-1} at room temperature on KBr pellets using an Avatar 370 from Nicolet. The chemical oxidation state was investigated by X-ray photoelectron spectra (XPS) from ThermoFisher Scientific with Al Kα radiation as the exciting source (300 W).

2.3. Catalytic degradation experiment

In this work, all the RhB degradation experiments were carried out in 1-L flask under mechanical stirring at a temperature approximately 25℃ without adjusting pH unless specified elsewhere. The time of catalyst and persulfate addition was considered as the beginning of reaction. At scheduled time intervals, 5 mL of the solution was taken out from the reactor as samples, and then, excess $NaNO_2$ was added into the samples for consuming the residual $S_2O_8^{2-}$ to prevent further reaction. Finally, $Fe_2(MoO_4)_3$ solid particles were removed by centrifuging and the supernatant was analyzed.

2.4. Analytical methods

The supernatant concentration was measured at 552 nm by UV–vis spectrophotometry (UNICO, UV-2100), and the UV–vis absorption spectra of supernatants were also recorded. The total organic carbon (TOC) was determined by Analyfik Jena AGN/C 2100 instrument. The measurements of iron ion concentration in solution followed UV–vis spectrophotometry at 665 nm.

The intermediates generated during RhB degradation were detected by GC/MC (Agilent 5775C, USA) as following The pre-treatment: the pH of 25 mL reacted solution was adjusted to 2 with 10% HCl, and the solution was extracted with 25 mL dichloromethane for three times. The total extract flowed through anhydrous sodium to remove water, and the

dehydrated solution was concentrated to 1 mL by rotatory evaporator. 0.5 mL bis(trimethylsilyl)trifluoroacetamide (BSTFA) was added into the concentrate, and then, trimethylsilylation of the total solution was implemented under 50℃ circumstance for 30 min. Finally, 1.0 μL sample was injected into GC with following temperature programming mode: The initial temperature 40℃ was maintained for 4 min, ramping to 80℃ (10℃/min rate) and held for 2 min, finally rise up to 280℃ (10℃/min rate), which was held for 10 min.

3. Results and discussion

3.1. Characterization of $Fe_2(MoO_4)_3$

The synthesized $Fe_2(MoO_4)_3$ is characterized via the wide-angle XRD patterns and FTIR spectroscopy. Fig. 1(a) illustrates that the main peaks appeared at 2θ of 20.48˚, 21.80˚, 23.00˚, 25.02˚, 25.76˚, 27.54˚, 30.22˚, and 34.1˚ and no peaks of other substances such as MoO_3 and Fe_2O_3 were observed, indicating the catalyst synthesized by co-precipitation method consisted of single phases, which were almost the same as the previously reported data for $Fe_2(MoO_4)_3$ [16].

The FTIR spectroscopy of $Fe_2(MoO_4)_3$ is shown in Fig. 1(b). The hydroxyl groups on $Fe_2(MoO_4)_3$ surface devoted the obvious peak at 3,420 cm^{-1}. The peaks at 840.70 and 600 cm^{-1} represented the vibrance of Mo–Fe and Fe–O [20], respectively. The peak at 1,039 cm^{-1} corresponded to the Fe–O–Mo [21] vibrance in the catalyst.

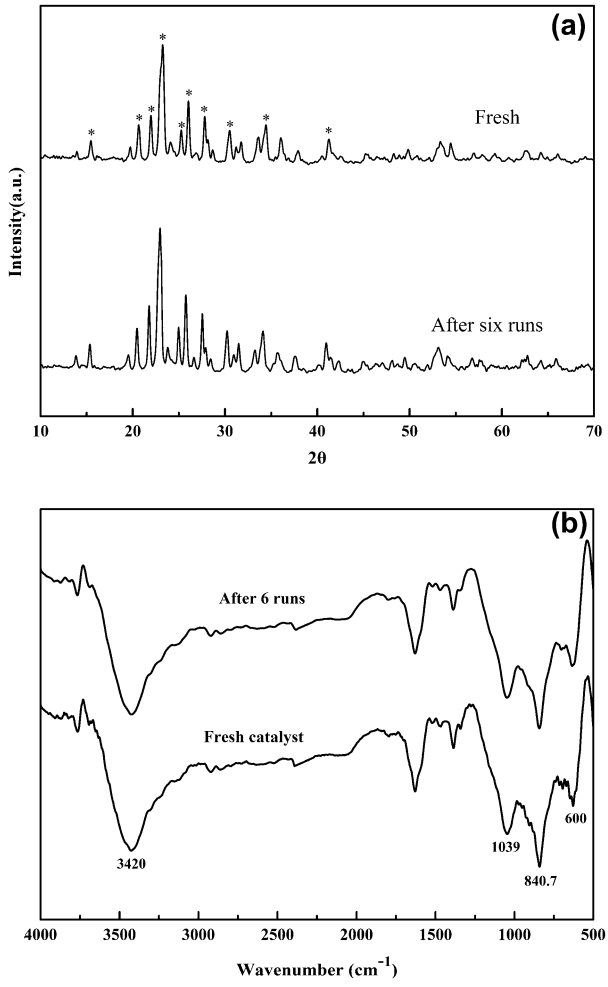

Fig. 1. XRD patterns (a) and FTIR spectra (b) of $Fe_2(MoO_4)_3$.

3.2. RhB degradation in $Fe_2(MoO_4)_3$/PS system

The RhB degradation in three different systems, $Fe_2(MoO_4)_3$, PS, and $Fe_2(MoO_4)_3$/PS, is introduced in Fig. 2. The results showed that when only $Fe_2(MoO_4)_3$ or PS in reaction system, RhB degradation was 2 and 60.16%, respectively. It could achieve about 99.01% in the presence of both $Fe_2(MoO_4)_3$ and PS. Although achieving high degradation efficiency in only PS system, no significant discoloration was observed, demonstrating that persulfate itself could not completely mineralize RhB. But in $Fe_2(MoO_4)_3$/PS system, the RhB degradation efficiency was obvious, accompanied by significant fading, which might be caused by the activation of persulfate.

In this section, main influencing factors, such as initial RhB concentration, PS concentration, $Fe_2(MoO_4)_3$ load, and initial pH, were performed to clarify the effects on the RhB degradation.

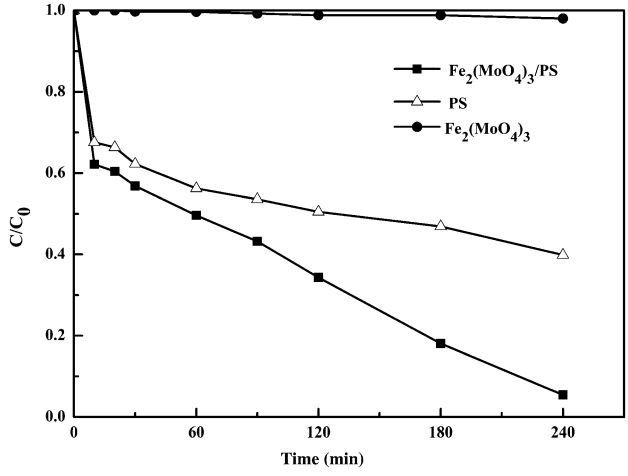

Fig. 2. The removal of RhB in different systems. Reaction conditions: RhB concentration 10.0 mg/L, $Fe_2(MoO_4)_3$ load 0.4 g/L, PS concentration 4 mM.

3.2.1. Effect of RhB initial concentration

It is important in the process of wastewater treatment to investigate the effect of the initial pollutant concentration. Fig. 3(a) shows the dye efficiencies at various RhB initial concentrations. It decreased from 98.09 to 85.58% with increasing RhB initial concentrations from 10 to 50 mg/L. It was apparent that the higher the initial concentration, the lower the molar ratio of $SO_4^{\cdot-}$/RhB, as the $SO_4^{\cdot-}$ produced would be constant under the same concentration of $Fe_2(MoO_4)_3$ and persulfate. Therefore, RhB solution with lower initial concentration was more likely to be degraded. Moreover, the data for RhB degradation were further analyzed by kinetic equation and followed the first-order kinetic model $\ln(C/C_0) = -kt$, where k is the rate constant, C_0 and C are the RhB concentration at $t = 0$ and time t, respectively. When RhB concentration increased from 10 to 50 mg/L, the reaction rate constant decreased from 1.51×10^{-2} to 0.75×10^{-2} min^{-1}, consistent with the degradation efficiencies (Fig. 4(a)).

3.2.2. Effect of persulfate and catalyst concentration on catalytic activity

The influence of PS concentration on RhB degradation process is presented in Fig. 3(b). It was found that the PS concentration was higher and the greater degradation efficiency was obtained. RhB degradation reached 55.45% (2 mM PS) and increased to 94.57% at 6 mM PS, since $S_2O_8^{2-}$ was the main driving force to generate $SO_4^{\cdot-}$ in this system. The rate constant k also increased from 0.28×10^{-2} to 1.00×10^{-2} min^{-1} with

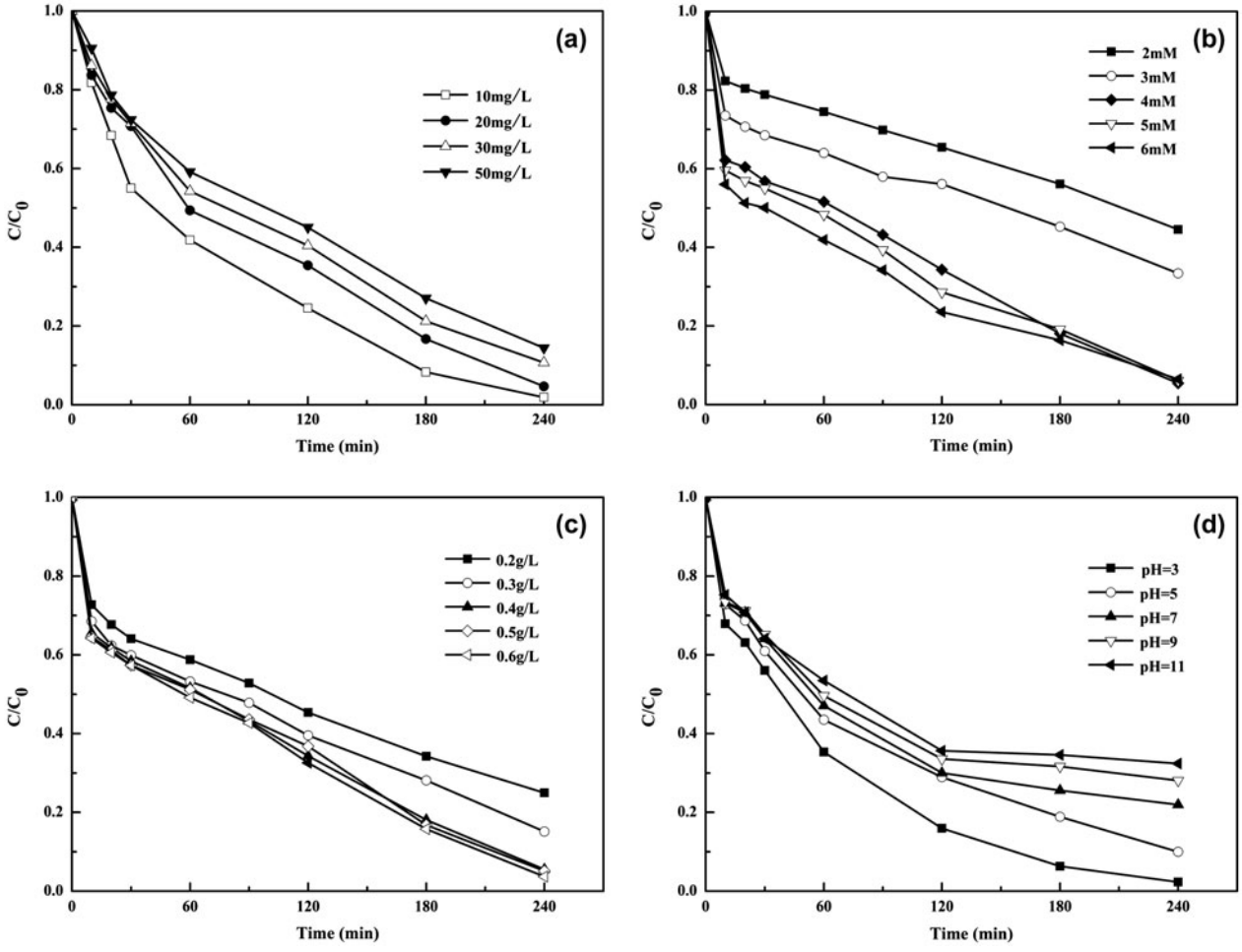

Fig. 3. Effects of (a) RhB initial concentration, (b) PS concentration, (c) $Fe_2(MoO_4)_3$ load and (d) initial pH on degradation efficiencies. Reaction conditions: (a) $Fe_2(MoO_4)_3$ load 0.4 g/L, PS concentration 4 mM, (b) RhB concentration 10.0 mg/L, $Fe_2(MoO_4)_3$ load 0.4 g/L, (c) RhB concentration 10.0 mg/L, PS concentration 4 mM, and (d) RhB concentration 10.0 mg/L, $Fe_2(MoO_4)_3$ load 0.4 g/L, PS concentration 4 mM.

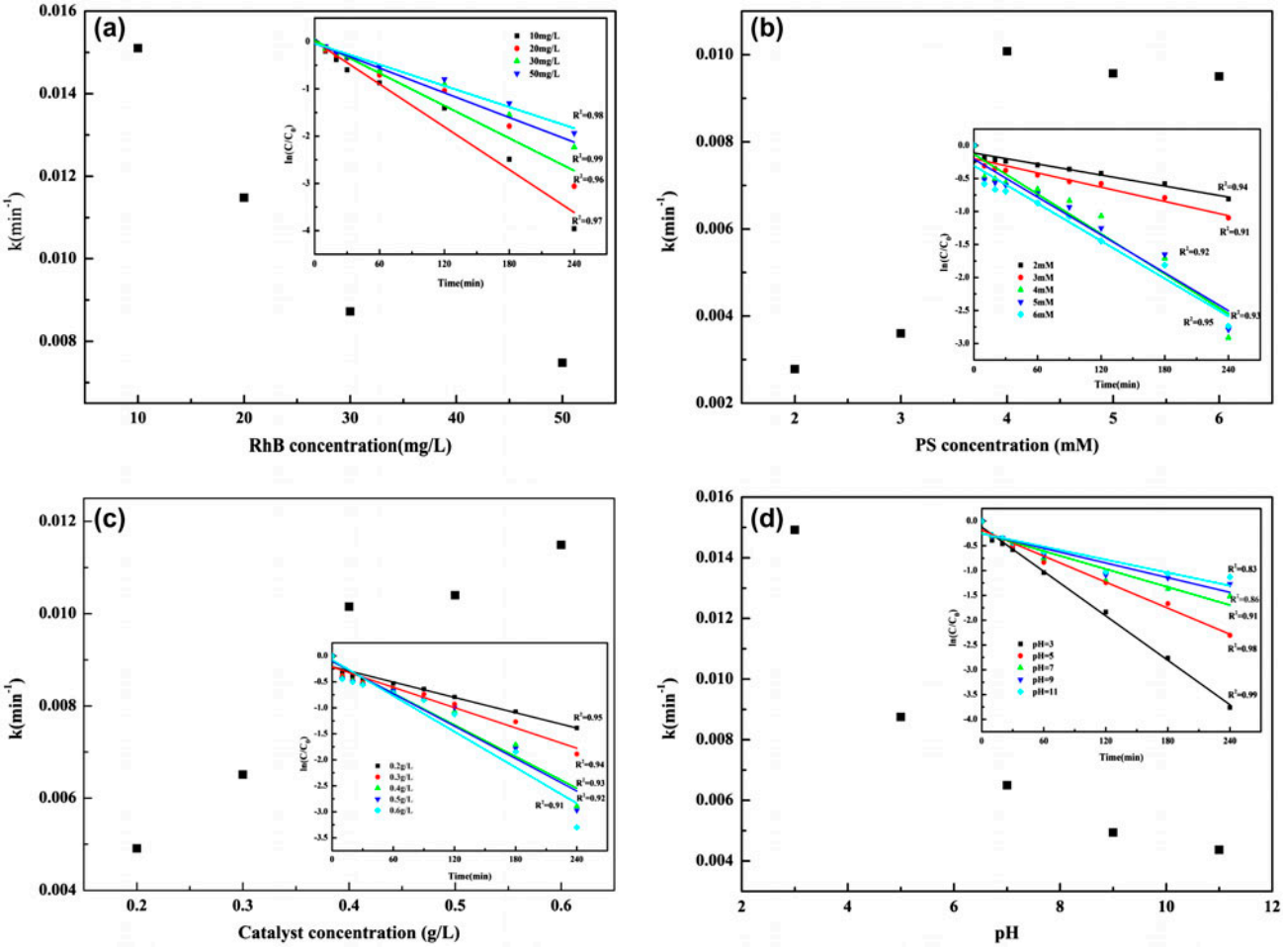

Fig. 4. Effect of (a) RhB initial concentration on the rate constant, (b) PS concentration, (c) catalyst concentration, and (d) initial pH on the rate constant of RhB degradation.

increasing PS concentration from 2 to 4 mM (Fig. 4(b)). However, it was observed that the increase of RhB degradation was little when PS concentration was higher than 4 mM and k was slightly reduced from 1.00×10^{-2} to 0.95×10^{-2} min^{-1}. It was mainly because when PS concentration reached a certain value, it was high enough for a given $Fe_2(MoO_4)_3$ load, and the influence of PS concentration on RhB degradation would become less. What's more, superfluous PS could be scavenger and react with SO_4^{-} to form SO_4^{2-} [22].

In the meanwhile, the RhB degradation increased from 75.06 to 96.31% with increasing $Fe_2(MoO_4)_3$ load (Fig. 3(c)). RhB degradation also followed the pseudo-first-order kinetics with the reaction rate increasing from 0.49×10^{-2} to 1.15×10^{-2} min^{-1} (Fig. 4(c)). However, the degradation trend was not significant. The reason was that enhanced $Fe_2(MoO_4)_3$ load would provide more catalytic active sites for the activation of persulfate to generate more sulfate radicals. But when persulfate concentration was constant, there was a certain competition for $S_2O_8^{2-}$ between Fe^{3+} and MoO_4^{2-} in $Fe_2(MoO_4)_3$ [16], indicated persulfate concentration was the main factors in this system.

3.2.3. Effect of initial pH on catalytic activity

The RhB degradation was evaluated at various pH in $Fe_2(MoO_4)_3$/PS system, and the results are displayed in Fig. 3(d). The RhB degradation efficiencies declined with increasing pH value and the highest degradation (almost 100%) was obtained when initial pH was 3.0. It could achieve 84.72% under the neutral environment and was high as 64.56% at pH 11. Hence, $Fe_2(MoO_4)_3$ displayed high catalytic activity toward persulfate for RhB degradation in a wide

range of pH. It could be explained by the solid acid characteristics of $Fe_2(MoO_4)_3$, which were the low PZC and strong acid sites. The low PZC of $Fe_2(MoO_4)_3$ could easily lead to the occurrence of deprotonation, and an acidic microenvironment was formed near the surface of $Fe_2(MoO_4)_3$ particles [16]. Additionally, sulfate radicals could react with hydroxyl in the solution to generate hydroxyl radicals. Compared with $SO_4^{\cdot-}$, $^{\cdot}OH$ is known to be unselective due to its high reactivity with various organic and inorganic species and more readily to be scavenged by non-target species. Besides the short lifetime of $SO_4^{\cdot-}$ (4s) is much longer than $^{\cdot}OH$ (20 ns), $^{\cdot}OH$ cannot diffuse into the surface of organic matter for degradation in time and could be scavenged by CO_3^{2-} or HCO_3^- being present possibly in alkaline environment [23], thus making the degradation efficiency lessen and the reaction rate constant decreased from 1.49×10^{-2} to 0.44×10^{-2} min^{-1} (Fig. 4(d)).

3.2.4. UV–vis spectra and mineralization

Fig. 5(a) illustrates the UV–vis spectra of six samples during RhB degradation process in $Fe_2(MoO_4)_3$/PS system. Absorption spectrum of RhB solution was mainly characterized by the band located at 552 nm, due to the four ethylated groups existing in RhB molecule [24]. A gradual fading of the absorbance value at the characteristic band was found during the experiment, and almost 100% removal efficiency was obtained after 4 h reaction. Compared with the control sample, there were blue shift of the main chromophore band and no new bands appeared obviously in another samples. The gradual fading was mainly attributed to $SO_4^{\cdot-}$ attacking, which caused two competitive processes occurred simultaneously during RhB degradation [25,26], including N-deethylation and the destruction of dye chromophore structure. The blue shift might be ascribed to the intermediates of N-deethylation.

High degradation of RhB was quite untypical of being mineralized into CO_2 and H_2O, as reaction organic intermediates could be formed during oxidation. In order to explore the extent of mineralization, the TOC experiment was carried out since it is a suitable indicator of organic mineralization. As demonstrated in Fig. 5(b), TOC removal increased gradually when the reaction proceeded. Firstly, the reaction was carried out for 0.5 h and TOC removal rapidly reached

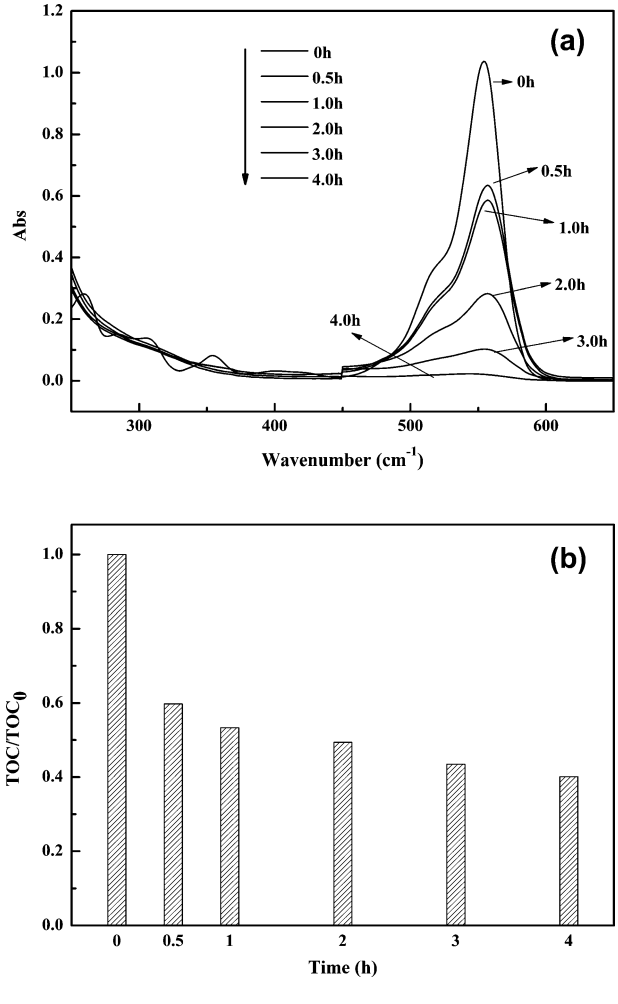

Fig. 5. UV–vis spectra (a) and TOC (b) removal of RhB degradation. Reaction conditions: RhB concentration 10.0 mg/L, $Fe_2(MoO_4)_3$ load 0.4 g/L, PS concentration 4 mM.

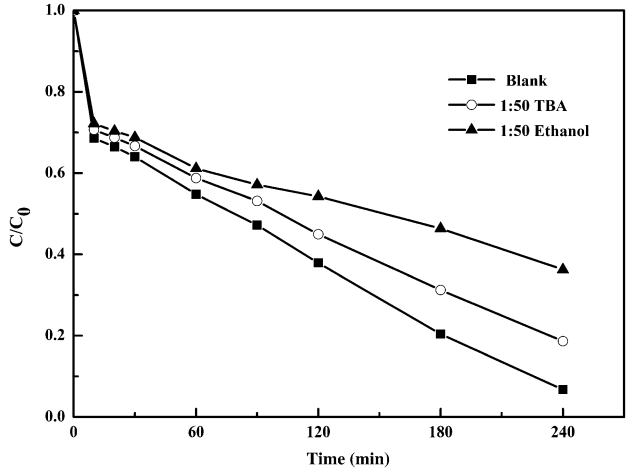

Fig. 6. Reaction of RhB in the presence of different radical scavengers. Reaction conditions: RhB concentration 10 mg/L, $Fe_2(MoO_4)_3$ load 0.4 g/L, PS concentration 4 mM.

36.25%. And then, it increased slowly, which was 46.66, 50.63, 56.58, and 59.88% after 1, 2, 3, and 4 h, respectively. RhB was destroyed completely but not fully mineralize, and for the reaction, organic intermediates were very difficult to be mineralized [27].

3.3. Identification of reactive radicals

Sulfate radicals in aqueous solution can result in radical inter-conversion reactions to produce hydroxyl radicals. Both $SO_4^{\cdot-}$ and $^{\cdot}OH$ have the strong oxidation ability for the destruction of organic contaminants. In order to confirm the generation of radicals species from $Fe_2(MoO_4)_3$/PS system, the tert-butyl alcohol (TBA, without R-hydrogen) was chosen as scavenger for $^{\cdot}OH$ and ethanol (EtOH, containing R-hydrogen) as scavenger for $SO_4^{\cdot-}$ and $^{\cdot}OH$, which was based on the different reaction rate constants between quencher and radicals [28,29]. EtOH reacts with $SO_4^{\cdot-}$ and $^{\cdot}OH$ at high comparable rates, which were 1.6–7.7 × 10^7 mol L^{-1} s^{-1} and 1.2–2.8 × 10^9 mol L^{-1} s^{-1}, respectively. However, the reaction rate of TBA and $^{\cdot}OH$ (3.8–7.6 × 10^8 mol L^{-1} s^{-1}) was 418–1,900 times faster than the rate of TBA and (4–9.1 × 10^5 mol L^{-1} s^{-1}) $SO_4^{\cdot-}$ [30,31].

TBA and EtOH indeed both inhibited RhB degradation in Fig. 6. When 0.2 mol/L TBA (molar ratio TBA/PS = 50) was introduced into $Fe_2(MoO_4)_3$/PS system, the degradation efficiency decreased to 86.36% after 240 min, created about 11.73% difference with regard to the blank value. On the other hand, the addition of 0.2 mol/L EtOH (molar ratio EtOH/PS = 50) resulted in decreased degradation efficiency of 36.34%. The loss of degradation efficiency caused by EtOH was relatively higher than that with TBA,

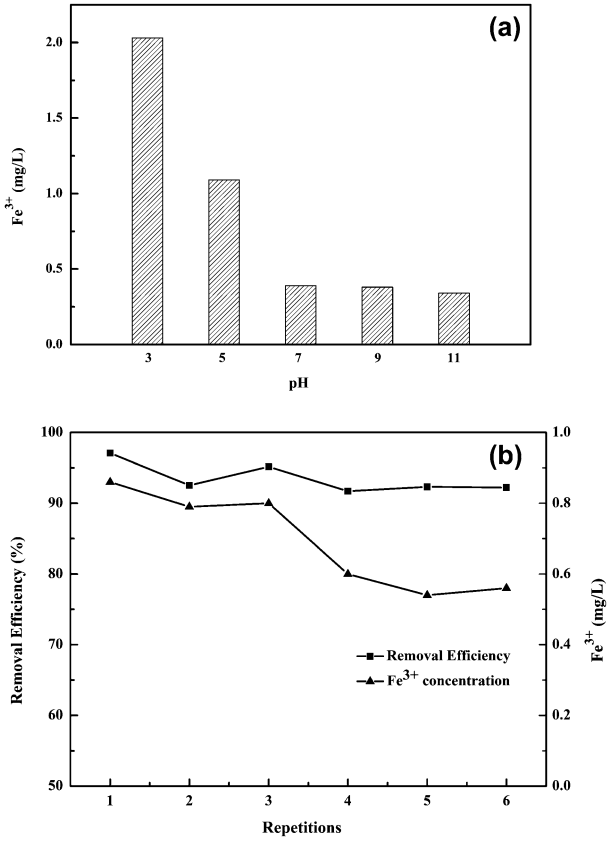

Fig. 7. Iron leaching under different initial pH (a) and regeneration times on RhB degradation. (b) Reaction conditions: RhB concentration 10 mg/L, $Fe_2(MoO_4)_3$ load 0.4 g/L, PS concentration 4 mM, reaction time 4 h.

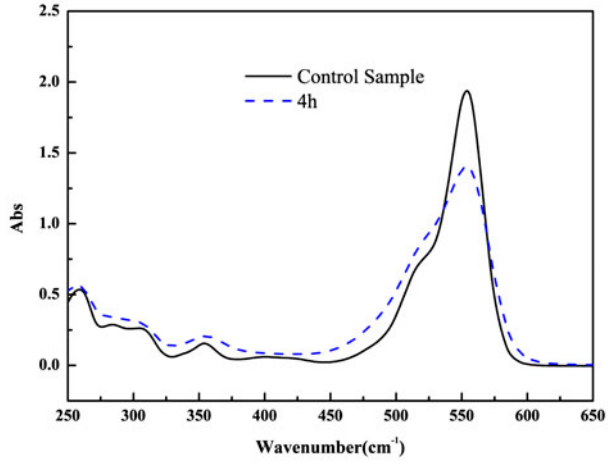

Fig. 8. The UV–vis spectra of RhB degradation in only PS system.

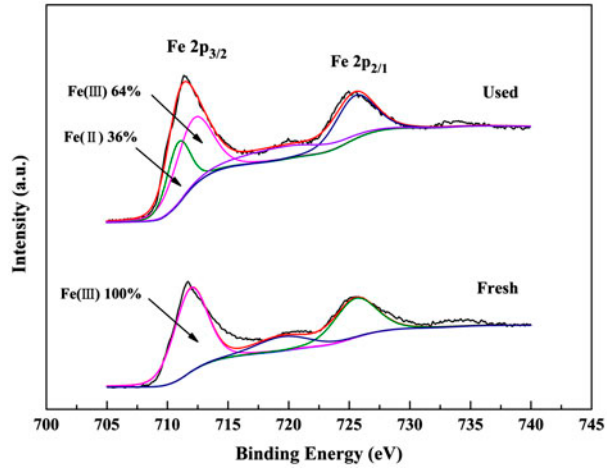

Fig. 9. XPS spectra of Fe 2p regions of fresh and used $Fe_2(MoO_4)_3$.

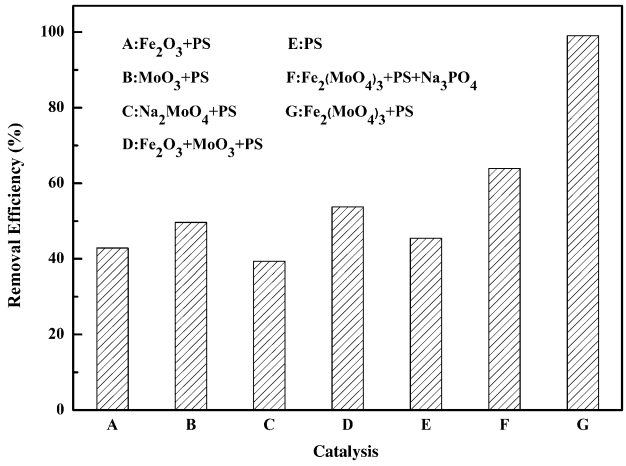

Fig. 10. Comparison of the catalytic activity of various compounds. Reaction conditions: RhB concentration 10 mg/L, $Fe_2(MoO_4)_3$ load 0.4 g/L, PS concentration 4 mM, reaction time 4 h.

indicated that $SO_4^{\cdot-}$ was predominantly produced over $^{\cdot}OH$ during the $Fe_2(MoO_4)_3$ for $S_2O_8^{2-}$ activation process without pH adjustment (about 5.6), while $^{\cdot}OH$ played a minor role in the degradation process.

3.4. Stability, reusability, and catalytic mechanism of $Fe_2(MoO_4)_3$

For a heterogeneous catalytic system, it is necessary to evaluate the stable performance of catalyst. Based on this purpose, the Fe leaching under different pH and reuse experiment were carried out. Fig. 7(a) shows the Fe leaching at various pH in $Fe_2(MoO_4)_3$/PS system, and Fe leaching concentration decreased slightly with increased pH. 2.24 mg/L concentration was the highest at pH 3, accounted for 2.9% in the total Fe content in $Fe_2(MoO_4)_3$. Therefore, it could be preferable to maintain a high catalytic activity for a heterogeneous catalyst, and persulfate could not be activated by leached Fe^{3+} directly.

In reusable experiments of the catalyst, the filtration was used to collect $Fe_2(MoO_4)_3$ after the degradation experiment. The collected catalyst was washed with double-distilled water for five times and dried under 105℃ environmental conditions, and the filtrate was used to determinate the leached Fe^{3+} concentration. The degradation efficiency of RhB for every reuse run almost was maintained unchanged, keeping the high activity during the 6 runs (Fig. 7(b)). When $Fe_2(MoO_4)_3$ was used for the sixth time, the RhB degradation efficiency was still over 90% in 4 h reaction. The results also showed that the leached Fe^{3+} concentration was in the range from 0.86 to 0.54 mg/L, which were below 2 mg/L (European Union), at most accounting for 0.898% when $Fe_2(MoO_4)_3$ was used firstly. The efficient RhB degradation and the little Fe^{3+} leaching indicated that $Fe_2(MoO_4)_3$ catalyst was durable and could be reused without loss of catalytic activity.

The chemical stability and efficient catalytic ability of $Fe_2(MoO_4)_3$ might be related to its high structure stability, which was confirmed by XRD and FTIR measurements on the used and fresh catalysts. The XRD patterns and FTIR spectroscopy of $Fe_2(MoO_4)_3$ after several times used confirmed that the structure of $Fe_2(MoO_4)_3$ did almost no change (Fig. 1).

It is believed that the mechanism in Fe^{2+}/PS system and heterogeneous Fe^{2+}/PS system is popular.

Table 1
Identification of intermediates during the oxidation degradation of RhB by GC/MS

Product	R_t (min)	M_w	Formula	Name
1	8.303	90	$C_4H_{10}O_2$	1,4-Butylene glycol
2	8.487	90	$C_2H_2O_4$	Acetic acid
3	8.875	76	$C_3H_8O_2$	1,2-Propylene glycol
4	9.249	136	$C_9H_{12}O$	1-p-Tolylethanol
5	10.054	62	$C_2H_6O_2$	Ethylene glycol
6	11.974	90	$C_3H_6O_3$	2-Hydroxypropanoic acid
7	15.664	192	$C_{11}H_{12}O_3$	4,7-Dimethoxyindan-1-one
8	16.023	92	$C_3H_8O_3$	Propane-1,2,3-triol
9	17.067	184	$C_8H_8O_5$	3,4-Dihydroxymandelic acid
10	19.352	122	$C_7H_6O_2$	3-Hydroxybenzoic acid
11	19.730	122	$C_8H_{10}O$	2,6-Dimethylphenol
12	23.442	166	$C_8H_6O_4$	Phthalic acid
13	24.411	278	$C_{16}H_{22}O_4$	Dibutyl phthalate
14	25.005	118	$C_4H_6O_4$	Succinic acid

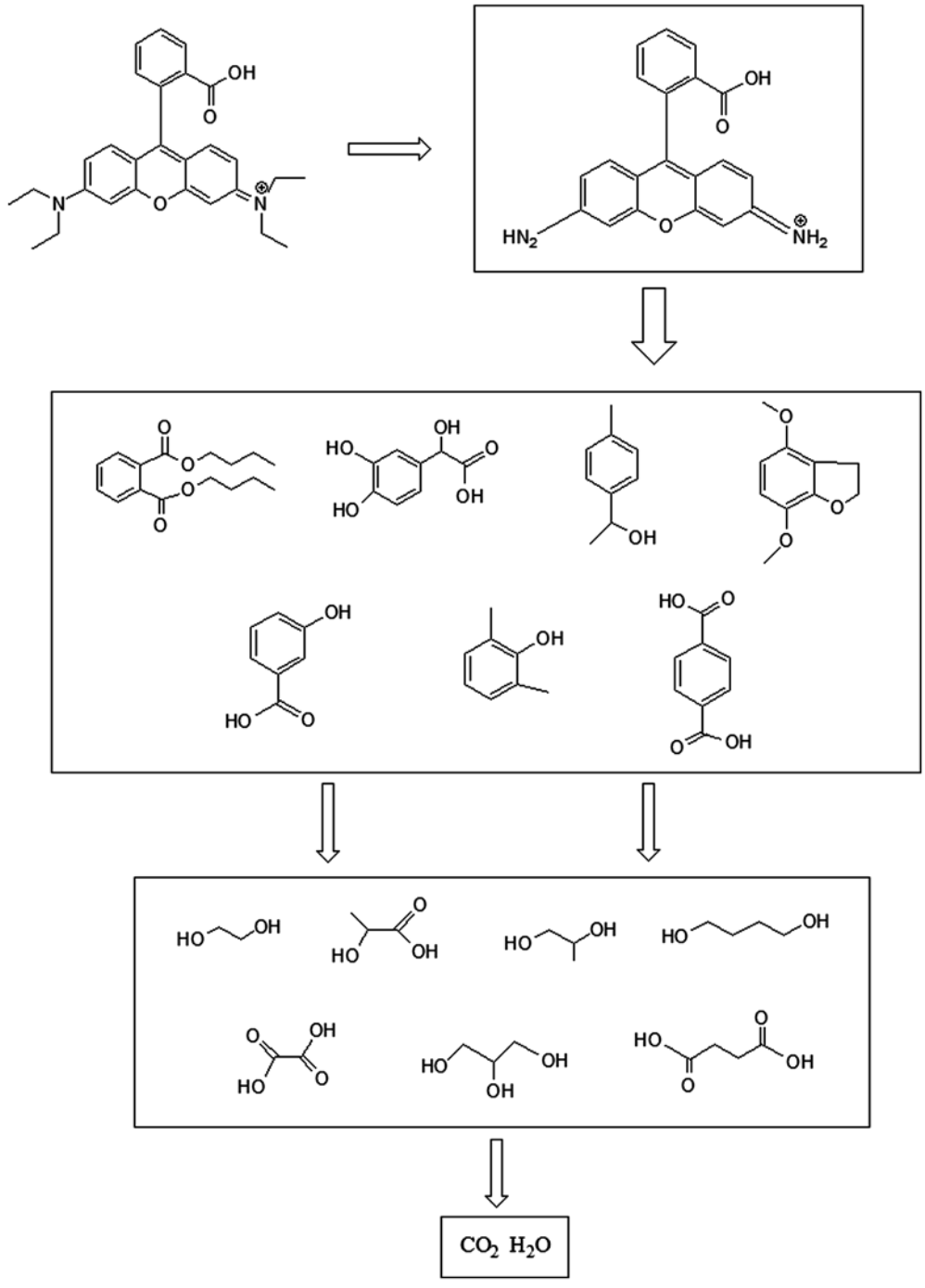

Fig. 11. Proposed pathway of RhB in $Fe_2(MoO_4)_3$/PS system.

$Fe_2(MoO_4)_3$ as a heterogeneous catalyst was used to activate PS for the efficient RhB removal in this study. As shown in Fig. 2, almost the same RhB removal was obtained at the beginning of the reaction in only PS system and $Fe_2(MoO_4)_3$/PS system and PS itself could be used as the oxidizing agent to oxidize RhB incompletely, producing some other organic compounds. Compared with the control sample, a small increase of absorbance was observed from 350 to 500 nm in the UV–vis spectra of RhB degradation by PS alone (Fig. 8) and this might correspond to quinone compounds [32], which could be as electron transfer agents aiming at reducing Fe(III) to Fe(II), and then generated Fe(II) could react with PS as an activator to form $SO_4^{\cdot-}$. In

the subsequent degradation process, large number of intermediates including hydroxybenzene and quinone compounds would be produced by $SO_4^{\cdot-}$, and hydroxybenzene was the same quinone and could be used as electron transfer agents [33,34]. Francesco Minisci [35] indicated that the $SO_4^{\cdot-}$ formed grabbed an electron from oxidized organics during the degradation process and then, oxidized organics might surrender to the organic compound radical, which could promote the Fe(III)/Fe(II) redox potential to generate Fe(II) by reacting with Fe(III). Therefore, activation of PS by Fe(II) generated could oxidize completely RhB, while Fe(II)was continuously produced from Fe(III)/Fe(II) recycled in $Fe_2(MoO_4)_3$ catalyst. To verify the Fe(III)/Fe(II) redox potential in catalytic oxidation, the XPS spectra of $Fe_2(MoO_4)_3$ before and after degradation experiment were recorded (Fig. 9). The peak of Fe $2p_{3/2}$ was at 711.7 eV for the fresh $Fe_2(MoO_4)_3$ catalyst, which was mainly contributed to Fe(III) [36]. After the degradation experiment, the binding energy of Fe $2p_{3/2}$ was slightly shifted to 711.4 eV value, proved the transformation of Fe(III) to Fe(II) occurred during the catalytic process. Based on the deconvolution of Fe 2p envelop, 36% Fe(II) came from Fe(III) reduction.

In order to clarify that there was synergistically catalytic effect between Fe^{3+} and MoO_4^{2-} in $Fe_2(MoO_4)_3$, we carried out comparable experiments using Na_2MoO_4 and Fe_2O_3 (Fig. 10). It was observed that the catalytic activity of $Fe_2(MoO_4)_3$ was much higher than that of Na_2MoO_4 and Fe_2O_3, proving that it actually existed a synergistically catalytic effect between Fe^{3+} and MoO_4^{2-} in $Fe_2(MoO_4)_3$.

Compared with $Fe_2(MoO_4)_3$/PS system, the dye degradation efficiency in $Fe_2(MoO_4)_3$/PS/Na_3PO_4 system was much lower (Fig. 10). This indicated that adding the phosphate could cause significant inhibition on RhB degradation, since surface hydroxyl groups could be substituted by phosphate owing to the stronger affinity between phosphate and active sites [37]. It was confirmed that the surface hydroxyl groups of $Fe_2(MoO_4)_3$ could be active sites for persulfate.

There was another possible mechanism existing between $Fe_2(MoO_4)_3$ and PS. MoO_4^{2-}/H_2O_2 system has been used in the catalytic oxidation, which could form the molybdenum (Mo) peroxo complex with strong oxidant for the organic compounds degradation directly. Tian [16] had verified that MoO_4^{2-} in $Fe_2(MoO_4)_3$ could catalyze H_2O_2 to generate the intermediate $MoO_2(O_2)_2^{2-}$. As persulfate and H_2O_2, both have the –O–O– band in their structure, speculating that persulfate could react with MoO_4^{2-} to generate molybdenum peroxo complex.

3.5. Possible degradation pathway of RhB

Analysis of the reaction intermediates and final products was useful for evaluating the efficiency of catalytic systems and may reveal the reaction process in details. The RhB degradation intermediates in $Fe_2(MoO_4)_3$/PS system were identified by GC/MS. According to GC/MS chromatograms, the major intermediates could be divided into two groups: the aromatic compounds with different substituent groups and the resultants with relatively lower molecular weights, which are shown in Table 1.

Based on the identification of GC/MS, seven benzenoid intermediates were identified including 1-p-tolylethanol, 4,7-dimethoxyindan-1-one, 3-hydroxybenzoic acid, 3,4-dihydroxymandelic acid, 2,6-dimethylphenol, phthalic acid, and dibutyl phthalate. The reaction between sulfate radicals and aromatic compound is usually considered to be the result of electron transfer. Benzene was attacked by sulfate radical losing an electron, formed unstable benzene radical. Then, the benzene was opened and further oxidized by $SO_4^{\cdot-}$ to form some lower molecular organic as listed in Table 1. Corresponding to GC/MS identification data, the possible degradation pathway of RhB in $Fe_2(MoO_4)_3$/PS system is depicted in Fig. 11.

4. Conclusions

Results of this study demonstrated that $Fe_2(MoO_4)_3$ as a novel heterogeneous catalyst had high efficient activity, excellent stability, and strong reusability. In $Fe_2(MoO_4)_3$/PS system, 10 mg/L RhB could be completely removed and 59.88% TOC removal efficiency was achieved under the addition of 4 mM $S_2O_8^{2-}$ and 0.4 g/L $Fe_2(MoO_4)_3$ within 240 min. Fe(III)/Fe(II) recycled, synergistically catalytic effect, and surface hydroxyl groups in $Fe_2(MoO_4)_3$ played important roles in the catalytic mechanism for persulfate. Based on GC/MS analysis, the major intermediates of RhB were identified and the degradation pathway of RhB was proposed. These revealed that $Fe_2(MoO_4)_3$/PS system has great potential in printing and dyeing wastewater and other refractory organic toxic pollutants treatment.

Acknowledgments

Financially, this work was supported by the Shanghai Committee of Science and Technology (Grant No. 12231202004). The authors also appreciate the technical support from Instrumental Analysis & Research Center of Shanghai University.

References

[1] A.D. Bokare, W. Choi, Review of iron-free Fenton-like systems for activating H_2O_2 in advanced oxidation processes, J. Hazard. Mater. 275 (2014) 121–135.

[2] A. Babuponnusami, K. Muthukumar, A review on Fenton and improvements to the Fenton process for wastewater treatment, J. Environ. Chem. Eng. 2 (2014) 557–572.

[3] K. Govindan, M. Raja, M. Noel, E.J. James, Degradation of pentachlorophenol by hydroxyl radicals and sulfate radicals using electrochemical activation of peroxomonosulfate, peroxodisulfate and hydrogen peroxide, J. Hazard. Mater. 272 (2014) 42–51.

[4] G.P. Anipsitakis, D.D. Dionysiou, Degradation of organic contaminants in water with sulfate radicals generated by the conjunction of peroxymonosulfate with cobalt, Environ. Sci. Technol. 37 (2003) 4790–4797.

[5] C.W. Wang, C. Liang, Oxidative degradation of TMAH solution with UV persulfate activation, Chem. Eng. J. 254 (2014) 472–478.

[6] M. Nie, Y. Yang, Z. Zhang, C. Yan, X. Wang, H. Li, W. Dong, Degradation of chloramphenicol by thermally activated persulfate in aqueous solution, Chem. Eng. J. 246 (2014) 373–382.

[7] Y.F. Rao, L. Qu, H. Yang, W. Chu, Degradation of carbamazepine by Fe(II)-activated persulfate process, J. Hazard. Mater. 268 (2014) 23–32.

[8] X. Jiang, Y. Wu, P. Wang, H. Li, W. Dong, Degradation of bisphenol A in aqueous solution by persulfate activated with ferrous ion, Environ. Sci. Pollut. Res. 20 (2013) 4947–4953.

[9] J. Deng, Y. Shao, N. Gao, Y. Deng, C. Tan, S. Zhou, Zero-valent iron/persulfate(Fe^0/PS) oxidation acetaminophen in water, Int. J. Environ. Sci. Technol. 11 (2013) 881–890.

[10] J. Yan, M. Lei, L. Zhu, M.N. Anjum, J. Zou, H. Tang, Degradation of sulfamonomethoxine with Fe_3O_4 magnetic nanoparticles as heterogeneous activator of persulfate, J. Hazard. Mater. 186 (2011) 1398–1404.

[11] Y. Leng, W. Guo, X. Shi, Y. Li, A. Wang, F. Hao, L. Xing, Degradation of Rhodamine B by persulfate activated with Fe_3O_4: Effect of polyhydroquinone serving as an electron shuttle, Chem. Eng. J. 240 (2014) 338–343.

[12] L. Zhu, Z. Ai, W. Ho, L. Zhang, Core–shell Fe-Fe_2O_3 nanostructures as effective persulfate activator for degradation of methyl orange, Sep. Purif. Technol. 108 (2013) 159–165.

[13] J. Yan, L. Zhu, Z. Luo, Y. Huang, H. Tang, M. Chen, Oxidative decomposition of organic pollutants by using persulfate with ferrous hydroxide colloids as efficient heterogeneous activator, Sep. Purif. Technol. 106 (2013) 8–14.

[14] S.-Y. Oh, S.-G. Kang, D.-W. Kim, P.C. Chiu, Degradation of 2,4-dinitrotoluene by persulfate activated with iron sulfides, Chem. Eng. J. 172 (2011) 641–646.

[15] Y. Anjaneyulu, N. Sreedhara Chary, D. Samuel Suman Raj, Decolourization of industrial effluents—Available methods and emerging technologies—A review, Rev. Environ. Sci. Bio/Technol. 4 (2005) 245–273.

[16] S.H. Tian, Y.T. Tu, D.S. Chen, X. Chen, Y. Xiong, Degradation of acid orange II at neutral pH using $Fe_2(MoO_4)_3$ as a heterogeneous Fenton-like catalyst, Chem. Eng. J. 169 (2011) 31–37.

[17] H. Shi, X. Wang, R.M. Hua, Z. Zhang, J. Tang, Epoxidation of α,β-unsaturated acids catalyzed by tungstate (VI) or molybdate(VI) in aqueous solvents: a specific direct oxygen transfer mechanism, Tetrahedron 61 (2005) 1297–1307.

[18] C. Peng, L. Gao, S. Yang, J. Sun, A general precipitation strategy for large-scale synthesis of molybdate nanostructures, Chem. Commun. (2008) 5601–5603.

[19] W.M. Shaheen, Thermal behaviour of pure and binary $Fe(NO_3)_3{\cdot}9H_2O$ and $(NH_4)_6Mo_7O_{24}{\cdot}4H_2O$ systems, Mater. Sci. Eng.: A 445–446 (2007) 113–121.

[20] A.A. Belhekar, S. Ayyappan, A.V. Ramaswamy, FT-IR studies on the evolution of different phases and their interaction in ferric molybdate—Molybdenum trioxide catalysts, J. Chem. Technol. Biotechnol. 59 (1994) 395–402.

[21] F. Trifirò, S. Notarbartolo, I. Pasquon, The nature of the active component in a Fe_2O_3 MoO_3 catalyst: II. Study of the variations occurring during high temperature treatment, J. Catal. 22 (1971) 324–332.

[22] Z.C.B. Xiao, Y. Yu, J.R. Barker, Free radical reactions involving $Cl^{\cdot}$, $Cl_2^{\cdot-}$, and $SO_4^{\cdot-}$ in the 248 nm photolysis of aqueous solutions containing $S_2O_8^{2-}$and Cl^-, J. Phys. Chem. 108 (2004) 295–308.

[23] Y. Deng, C.M. Ezyske, Sulfate radical-advanced oxidation process (SR-AOP) for simultaneous removal of refractory organic contaminants and ammonia in landfill leachate, Water Res. 45 (2011) 6189–6194.

[24] A. Martínez-de la Cruz, U.M.G. Pérez, Photocatalytic properties of $BiVO_4$ prepared by the co-precipitation method: Degradation of Rhodamine B and possible reaction mechanisms under visible irradiation, Mater. Res. Bull. 45 (2010) 135–141.

[25] T. Wu, G. Liu, J. Zhao, Photo assisted degradation of dye pollutants. V. Self-photosensitized oxidative transformation of Rhodamine B under visible light irradiation in aqueous TiO_2 dispersions, J. Phys. Chem. B 102 (1998) 5845–5851.

[26] Z. He, S. Yang, Y. Ju, C. Sun, Microwave photocatalytic degradation of Rhodamine B using TiO_2 supported on activated carbon: Mechanism implication, J. Environ. Sci. 21 (2009) 268–272.

[27] S. Yang, X. Yang, X. Shao, R. Niu, L. Wang, Activated carbon catalyzed persulfate oxidation of Azo dye acid orange 7 at ambient temperature, J. Hazard. Mater. 186 (2011) 659–666.

[28] H.W.S. Chen Ju Liang, Identification of sulfate and hydroxyl radicals in thermally activated persulfate, Ind. Eng. Chem. Res. 48 (2009) 5558–5562.

[29] W. Chu, Y.R. Wang, H.F. Leung, Synergy of sulfate and hydroxyl radicals in UV/$S_2O_8^{2-}$/H_2O_2 oxidation of iodinated X-ray contrast medium iopromide, Chem. Eng. J. 178 (2011) 154–160.

[30] P. Neta, Rate constants for reactions of inorganic radicals in aqueous solution, J. Phys. Chem. Ref. Data 17 (1988) 1027–1284.

[31] G.V. Buxton, C.L. Greenstock, W.P. Helman, A.B. Ross, W. Tsang, Critical review of rate constants for reactions of hydrated electrons chemical kinetic data base for combustion chemistry. Part 3: Propane, J. Phys. Chem. Ref. Data 17 (1988) 513.

[32] A. Aguiar, A. Ferraz, Fe^{3+}- and Cu^{2+}-reduction by phenol derivatives associated with Azure B degradation in Fenton-like reactions, Chemosphere 66 (2007) 947–954.
[33] W.J.C. Christopher, K. Duesterberg, T. David Waite, Fenton-mediated oxidation in the presence and absence of oxygen, Environ. Sci. Technol. 39 (2005) 5052–5058.
[34] J.J.P. Ruzhong Chen, Role of quinone intermediates as electron shuttles in Fenton and photoassisted Fenton oxidations of aromatic compounds, Environ. Sci. Technol. 31 (1997) 2339–2406.
[35] A.C. Francesco Minisci, Electron-transfer processes peroxydisulfate, a useful and versatile reagent in organic chemistry, Acc. Chem. Res. 16 (1983) 27–32.
[36] Y. Wang, H. Zhao, M. Li, J. Fan, G. Zhao, Magnetic ordered mesoporous copper ferrite as a heterogeneous Fenton catalyst for the degradation of imidacloprid, Appl. Catal. B: Environ. 147 (2014) 534–545.
[37] T. Zhang, C. Li, J. Ma, H. Tian, Z. Qiang, Surface hydroxyl groups of synthetic α-FeOOH in promoting OH generation from aqueous ozone: Property and activity relationship, Appl. Catal. B: Environ. 82 (2008) 131–137.